Journal of the Argentine Chemical Society

DENSITY FUNCTIONAL THEORY (DFT) STUDY OF H_2S INTERACTIONS ON THE Pr-DOPED CeO_2(111) SURFACE

Alejandro Kinbaum[1], Eduardo Poggio-Fraccari[1,2], Fernando Mariño[1,2], Beatriz Irigoyen[1,2*]

[1] *UBA. Dto. de Ingeniería Química, Ciudad Universitaria, (1428) Buenos Aires, Argentina.*

[2] *CONICET- UBA, I. de Tec. del Hidrógeno y Energías Sostenibles (ITHES). Buenos Aires, Argentina.*

** Corresponding author. E-mail: beatriz@di.fcen.uba.ar*

Received February 27th, 2017. Approved April 18th, 2017.

Abstract

In this work, we performed a density functional theory (DFT) study of the H_2S interactions on a low praseodymium (Pr)-doped CeO_2(111) surface. For this study, we considered a 3.7 at% Pr doping and conducted DFT calculations using the GGA formalism with the 'U' correction on Ce(4f) and Pr(4f) orbitals. The H_2S molecule weakly interacts on both the stoichiometric and oxygen deficient (111) surface of undoped CeO_2 (ceria). However, on the $Ce_{0.963}Pr_{0.037}O_2$(111) surface with an oxygen vacancy (O-hole site near to Pr dopant), the presence of praseodymium promotes the dehydrogenation process with formation of HS and H species.

Resumen

En este trabajo presentamos un estudio basado en la teoría del funcional de la densidad (density functional theory, DFT) de las interacciones del H_2S sobre la superficie CeO_2(111) dopada con un bajo contenido de praseodimio (Pr). Para este estudio, se consideró un dopado de 3,7 at% de Pr y se efectuaron cálculos DFT usando el formalismo GGA e introduciendo la corrección 'U' sobre los orbitales Ce(4f) y Pr(4f). La molécula H_2S interactúa débilmente en la superficie CeO_2(111) sin dopar, tanto estequiométrica como deficiente de oxígeno. Sin embargo, en la superficie $Ce_{0.963}Pr_{0.037}O_2$(111) con una vacancia de oxígeno (sitio O-hole cerca del dopante Pr), la presencia de praseodimio promueve el proceso de deshidrogenación con la formación de las especies HS y H.

Palabras Clave: *Sulfuro de hidrógeno; Óxido de cerio; Praseodimio; Cálculos DFT+U*

Keywords: *Hydrogen sulfur; Cerium oxide; Praseodymium; DFT+U calculations*

1. Introduction

In the last decades, the search for new energy sources and alternative fuels are mainly forced by increasing concerns related to greenhouse gas emissions, finite availability of fossil combustibles, as well as health and safety considerations [1–3]. Hydrogen (H_2) is considered an environmentally friendly fuel and it can be produced from renewable resources such as biomass with low pollution and high efficiency.

Algae biomass has several advantages compared to other renewable energy sources: increased growing speed, high yield per surface unit [4], very efficient capture of carbon dioxide [5] and solar energy conversion [6], no-competence with the biomass used for food, and the possibility of growing in open waters [7]. Moreover, microalgae can employ the nutrients present in liquid urban residues to grow and, at the same time, pre-treating them [8].

Gasification of the algae biomass releases a stream containing CH_4, H_2, CO, CO_2, hydrocarbons of low molecular weight as well as several compounds with sulfur and nitrogen. This stream can be transformed into syngas (CO and H_2) and even improve its H_2 content through catalytic processes. However, these transformations involve not only CH_4 reforming but also prevention of catalysts deactivation by poisoning with sulfur-containing species.

Sulfur has a high negative impact on the several catalysts employed in industrial processes [9,10]. This negative effect can be mitigated removing most of the sulfur-containing species with hydro desulfurization catalysts or oxide adsorbents [11], but the associated energetic cost is very high. On the other hand, development of new catalysts with high sulfur tolerance represents an easier and less expensive alternative [12].

Sulfur is a poison for the metals of group VIII and especially causes severe deactivation of nickel [13]. Indeed, all the sulfur presents as H_2S can easily chemisorb on available Ni sites under CH_4 reforming reaction conditions.

As regard of Ni supports, Al_2O_3 is one of the most employed for Ni-based catalysts [14]. Particularly, better performance and sulfur tolerance has been reported for those Ni and noble metal catalysts supported on CeO_2 and CeO_2-ZrO_2 mixed oxides [15]. These features are mainly attributed to the good oxygen donation ability of CeO_2, originated by an easy transition of Ce cations oxidation state from Ce^{4+} to Ce^{3+} [16].

Therefore, the stability and catalytic performance of Ni active phase can be substantially improved by using a support based on CeO_2 [17]. In this regard, it is worth to note that the addition of praseo-

dymium into ceria lattice remarkably improves the oxygen storage capacity (OSC) of CeO_2 [18]. Thus, Pr-doped CeO_2 materials would promote the oxidation of H_2S, the most common sulfur-containing species and, so, be useful supports for the Ni active phase by preventing its deactivation due to sulfur poisoning.

By the way, as far as we know there are no previous theoretical studies of H_2S interactions on Pr-doped CeO_2 solid solutions. Therefore, in this work we performed density functional theory (DFT) calculations to evaluate H_2S interactions on a low Pr-doped CeO_2(111) surface.

2. Theoretical Methods

Cerium oxide (CeO_2, *ceria*) crystallizes in fluorite structure consisting of a face-centered cubic (fcc) system of Ce^{4+} cations with O^{2-} anions filling its tetrahedral holes. Experimental data indicated a lattice parameter value of 5.41 Å for this structure [19].

Concerning our work, optimization of the ceria bulk structure within a plane wave basis cutoff energy of 480 eV, led to a calculated lattice constant value of 5.50 Å. Then, the ideal model of the CeO_2 surface was constructed by cleaving the optimized bulk cell with the (111) plane and retaining an extra oxygen layer. We choose the (111) surface because it is the most stable among the low-index (111), (110) and (100) ones, and corresponds to minimal Ce–O bonds cleavage [20–22]. After that, the low-doped Pr-ceria surface was obtained from a CeO_2(111) slab, with a p(3x3) expansion of the surface unit cell, by substituting one surface Ce cation by Pr. This substitution allowed us to build the 3.7 at% Pr-doped CeO_2(111) surface.

Figure 1, shows the resulting $Ce_{0.963}Pr_{0.037}O_2$(111) surface. So, we can see the upper three atomic layers, an O-Ce-O sandwich formed by top O anions, surface Ce cations and subsurface O anions.

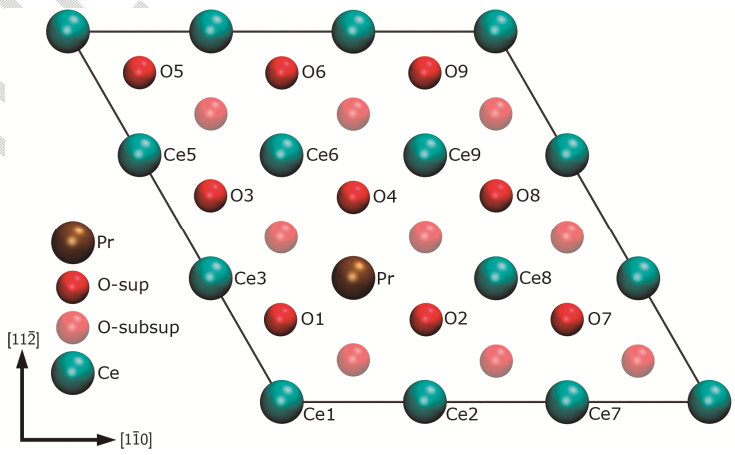

Figure 1. Front view of the stoichiometric $Ce_{0.963}Pr_{0.037}O_2$(111) surface.

The density functional theory (DFT) calculations were performed with the Vienna Ab-initio Simulation Package (VASP) [23,24]. The Kohn-Sham equations were solved with the generalized gradient approximation (GGA), and the exchange correlation functional of Perdew-Burke-Ernzerhof (PBE). Geometries were optimized until the Hellmann-Feynman forces converged to less than 0.02 eV/Å. The cutoff energy of the plane wave basis was set to 480 eV, and the core electrons were represented with the projector augmented wave (PAW) method using Ce($5s^2$, $5p^6$, $6s^2$, $5d^1$, $4f^1$), Pr($5s^2$, $5p^6$, $6s^2$, $5d^1$, $4f^2$) and O($2s^2$, $2p^4$) configurations for valence electrons. Self-consistent calculations were performed sampling the Brillouin zone with a 3×3×1 k-points grids under the Monkhorst-Pack scheme [25]. The different configurations were optimized using spin polarization calculations.

The standard DFT formulation usually fails to describe strongly correlated electrons in Ce(4f) and Pr(4f) orbitals, due to a deficient treatment of electron correlations. This limitation can be corrected to some extent by using the DFT + U method, where the introduction of a Hubbard parameter 'U' modifies the electron self-interaction error and enhances the description of the correlation effects. Accordingly, we used the Hubbard parameters: U_{eff} = 5 eV for Ce(4f) states, and U_{eff} = 4.5 eV for Pr(4f) orbitals. The value U_{eff} = 5 eV was chosen for the Ce(4f) states as it correctly described the atomic and electronic structure of both CeO_2 and CeO_{2-x} systems [26–28]. On the other hand, the value U_{eff} = 4.5 eV was considered reliable for describing the strong onsite Coulomb repulsion among Pr(3d) electrons, as it has shown to reproduce the experimentally available data for PrO_2 such as lattice constant and band gap [29].

Moreover, oxidation states and spin polarization were computed for different ions of interest by performing Bader charge and spin charge density analysis [30–32].

3. Results and Discussion

We began our study calculating the H_2S interactions on the stoichiometric $Ce_{0.963}Pr_{0.037}O_2$(111) surface. For this, we considered different active sites: surface O anions as well as Ce^{4+} and Pr^{4+} cations. As it can be seen in Fig. 1, surface O1, O3 and O6 sites have different cationic environment. The oxygen O1 is located inside a triangle formed by Ce and Pr cations (Ce1, Ce3 and Pr). The O3 anion is located near Pr, but surrounded by Ce cations (Ce3, Ce4 and Ce5). Meanwhile, O6 is also in the center of a triangle formed by Ce cations (Ce2, Ce5 and Ce6) but located far away from Pr.

Then, we evaluated H_2S interactions on the oxygen deficient $Ce_{0.963}Pr_{0.037}O_{2-x}$(111) surface, with O1 vacancy, by considering Pr (Pr^{3+}), Ce4 (Ce^{4+}) and Ce3 (Ce^{3+}) sites.

The H_2S adsorption energy (ΔE_{ads}) on the stoichiometric $Ce_{0.963}Pr_{0.037}O_2$(111) was computed as:

$$\Delta E_{ads} = E[H_2S/Ce_{0.963}Pr_{0.037}O_2(111)] - E[Ce_{0.963}Pr_{0.037}O_2(111)] - E[H_2S].$$

In this equation, $E[H_2S/Ce_{0.963}Pr_{0.037}O_2(111)]$ represents the total energy of the system formed after H_2S molecular interactions on the stoichiometric surface, $E[Ce_{0.963}Pr_{0.037}O_2(111)]$ is the total energy of the stoichiometric surface, and $E[H_2S]$ is that of the H_2S molecule in vacuum.

On the other hand, H_2S adsorption energy on the oxygen deficient $Ce_{0.963}Pr_{0.037}O_{2-x}(111)$ surface, with O1 vacancy, was calculated as:

$$\Delta E_{ads} = E[H_2S/Ce_{0.963}Pr_{0.037}O_{2-x}(111)] - E[Ce_{0.963}Pr_{0.037}O_{2-x}(111)] - E[H_2S].$$

In this equation, $E[H_2S/Ce_{0.963}Pr_{0.037}O_{2-x}(111)]$ represents the total energy of the system formed after H_2S interaction on the O-deficient surface, $E[Ce_{0.963}Pr_{0.037}O_{2-x}(111)]$ is the total energy of the O-deficient surface, and $E[H_2S]$ is that of the H_2S molecule in vacuum.

3.1 H_2S interactions on the stoichiometric $Ce_{0.963}Pr_{0.037}O_2(111)$ surface

Molecular H_2S interactions on the stoichiometric $Ce_{0.963}Pr_{0.037}O_2(111)$ are very weak. The interaction of H_2S on surface oxygen anions is a physisorption as indicated by the low adsorption energy value $\Delta E_{ads} = -0.14$ eV, and the long O–S distance which was calculated in 3.51 Å. The molecular interactions of H_2S on Ce2 (a Ce^{4+} cation near to Pr) or Ce4 (a Ce^{4+} cation close to Pr) are very similar as we calculated similar adsorption values for both physisorptions: $\Delta E_{ads} = -0.34$ eV, and Ce3–S and Ce4–S distances of 3.20 Å and 3.22 Å, respectively. For the Pr site, we calculated an H_2S adsorption energy $\Delta E_{ads} = -0.31$ eV and a Pr–S distance of 3.23 Å.

For comparison, we also computed H_2S interactions on the undoped $CeO_2(111)$ surface. The molecular interaction on a Ce site is also a physisorption ($\Delta E_{ads} = -0.21$ eV and d(Ce–S) = 3.20 Å). Meanwhile, we computed no interactions of the H_2S molecule on O sites ($\Delta E_{ads} = -0.01$ eV. Thus, we underline that our results indicating very weak interactions of H_2S molecule on Ce cations ($\Delta E_{ads} = -0.21$ eV) are in good agreement with previous reported energies values for adsorbed H_2S species on the $CeO_2(111)$ surface of about –0.1 eV [33].

Concerning the electronic structure of the stoichiometric $Ce_{0.963}Pr_{0.037}O_2(111)$ surface, Bader charge calculations for Ce and Pr cations gave values of 9.6e and 10.69e, respectively, and the computation of spin magnetization resulted in 0 B for Ce cations and 1.2 B for Pr one [18].

For the different optimized $H_2S/Ce_{0.963}Pr_{0.037}O_2(111)$ systems, our Bader charge and spin magnetization calculations show no changes of the surface electronic configuration which confirm the physisorptive character of molecular H_2S interactions on the stoichiometric $Ce_{0.963}Pr_{0.037}O_2(111)$ surface.

Thus, it is possible to assume that the H_2S molecule is weakly bound to both the undoped and Pr-doped stoichiometric $CeO_2(111)$ surface. The small calculated binding energy corresponds to a physisorption, and this H_2S weakly bond molecule could be considered as an intermediate to more stable species.

3.2 H_2S interactions on the $Ce_{0.963}Pr_{0.037}O_{2-x}(111)$ surface with a vacancy of O1

Praseodymium doping significantly reduces the energy required for anionic defects formation on the ceria surface. The calculated energy value for creation of the O1-defect on the $Ce_{0.963}Pr_{0.037}O_2(111)$ surface is about 1 eV [18], in agreement with that reported for the $Ce_{0.9688}Pr_{0.0312}O_{1.9688}$ bulk structure [34]. This finding agrees with the increase of oxygen vacancies concentration reported for Pr-doped CeO_2 solids [35–37].

The creation of the O1 vacancy on the $Ce_{0.963}Pr_{0.037}O_2(111)$ surface reflected in atomic relaxations of surface and subsurface ions. The distance from Ce1 cation to O1-hole was elongated ~ 10% compared to the Ce1–O1 bond length in the stoichiometric Pr-substituted $CeO_2(111)$ surface [18]. Similarly, Ce3 and Pr distances to O1-hole resulted 7% larger than those to O1. Cerium cations like Ce1, Ce3 and Pr also relaxed moving 0.25 Å, 0.19 Å and 0.20 Å, respectively, away from the O1-hole.

The electronic structure of $Ce_{0.963}Pr_{0.037}O_{2-x}(111)$ surface with the O1 vacancy was characterized trough Bader charge and spin polarization analyses. Bader charge calculations show 9.92e for the Ce3 cation and 10.96e for Pr one, indicating that the two electrons left in the solid after formation of O1-defect were transferred to the closest Ce cation (Ce3) and the Pr dopant [18]. Accordingly, spin magnetization values of Ce3(4f) and Pr(4f) orbitals were calculated in about 1 B and 2 B, respectively.

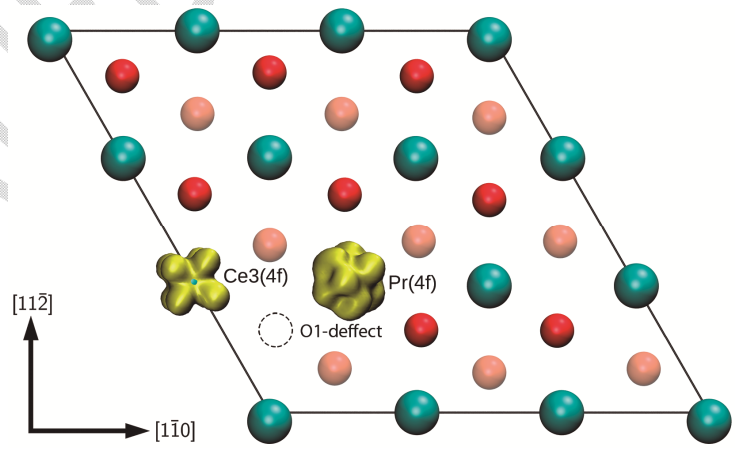

Figure 2: Electronic structure of the $Ce_{0.963}Pr_{0.037}O_{2-x}(111)$ surface with O1-defect. Spin polarization at a 0.05 e $Å^{-3}$ isovalue for Ce3(4f) and Pr(4f) orbitals. Positive and negative values are indicated in yellow and gray, respectively.

As regard of this electronic structure, Fig. 2 shows the isosurface of spin-polarized density for Ce3(4f) and Pr(4f) orbitals at a 0.05 e $Å^{-3}$ isovalue. As it can be seen, this isosurface also indicates that creation of O1-defect led to reduction of Pr and Ce3 cations.

Our study of H_2S interactions on the reduced $Ce_{0.963}Pr_{0.037}O_{2-x}(111)$ surface with an oxygen vacancy indicates that the H_2S molecule chemisorbed on the reduced cations. On the O-defective surface with a O1-hole, we computed strong adsorption energy values due to molecular H_2S interactions on Ce3 and Pr cations: $\Delta E_{ads} = -1.98$ eV on Pr^{3+} cation and $\Delta E_{ads} = -1.96$ eV on Ce3 (a Ce^{3+} cation). Together with these energy values, the distance between sulfur and Pr or Ce3 cations were calculated as follow: d(S–Pr) = 3.14 Å and d(S–Ce3) = 3.02 Å.

As well, we noticed that one of the H-S bonds was broken due to H_2S interaction on the O1-hole. Indeed, the first dehydrogenation of H_2S began with the molecule tilting towards the surface followed by the cleavage of one of the H–S bonds. Then, the process continues with the binding of this H fragment to the nearest oxygen anion and the sideways slipping of the HS species over the O1-hole.

Figure 3 displays the optimized atomic configuration for the HS-H/$Ce_{0.963}Pr_{0.037}O_{2-x}(111)$ system. Note that the HS fragment (d(H–S) = 1.35 Å) is over the O1-hole, while the H one is bound to lattice O^{2-} anion forming a hydroxyl species (d(H–O) =0.97 Å).

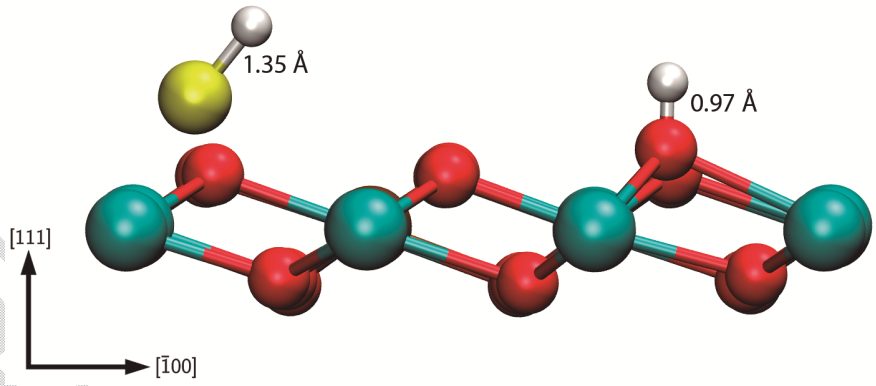

Figure 3: HS and H fragments adsorbed on the $Ce_{0,963}Pr_{0,037}O_{2-x}(111)$ surface with O1-defect

On the other hand, Bader charge calculations for the HS-H/$Ce_{0.963}Pr_{0.037}O_{2-x}(111)$ system indicate that only Ce3 (9.92e) and Pr (10.96e) are in the (3+) oxidation states. Accordingly, Ce and Pr cations show spin magnetizations of 1 B and 2 B, respectively. Thus, after adsorption of the HS and H fragments on the O-defective surface no new reduced cations were detected. This electronic struc-

ture is consistent with the isosurface of spin-polarized density shown in Fig. 4 for Ce3(4f) and Pr(4f) orbitals.

Altogether, our findings reveal a heterolytic cleavage of the H–SH bond into H^+ and HS^- species due to interaction of the H_2S molecule on the O-defective $Ce_{0.963}Pr_{0.037}O_{2-x}$(111) surface.

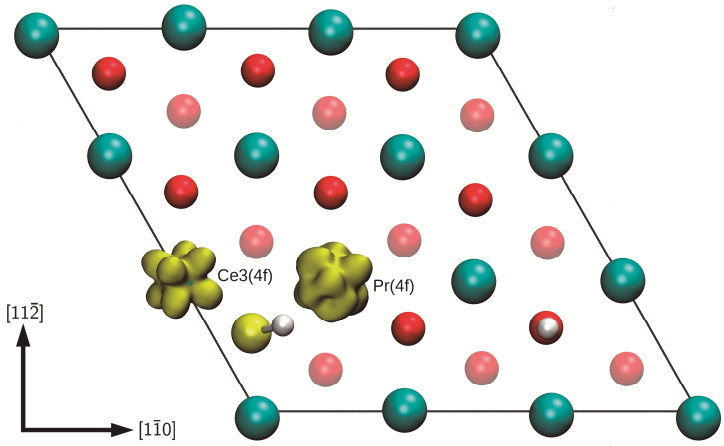

Figure 4: Electronic structure of the HS-H/$Ce_{0.963}Pr_{0.037}O_{2-x}$(111) system. Spin polarization at a 0.05 e $Å^{-3}$ isovalue for Ce3(4f) and Pr(4f) orbitals. Positive and negative values are indicatedin yellow and gray, respectively.

For completeness, we also calculated H_2S interactions on the CeO_{2-x}(111) surface with a vacancy of O1. The weak interaction of the molecule (ΔE_{ads} = –0.32 eV) suggests a physisorption. Besides, due to H_2S interaction on Ce3 cation one of the H–S bonds become elongated (d(H–S) = 1.48 Å). However, there was no cleavage of the molecule. In this regard, we emphasize that our results agree with previously reported DFT results indicating that H_2S interaction on the reduced CeO_{2-x}(111) surface is weak (ΔE_{ads} = –0.45 eV), and that it occurs via interaction between the sulfur atom of H_2S and the Ce atom nearest neighbor to the oxygen vacancy [38].

In summary, the DFT+U calculations performed in this work indicate that molecular adsorption of H_2S on both the stoichiometric and O-deficient undoped ceria (111) surface is unfavorable due to weak interactions between the H_2S molecule and the ceria surface. Moreover, this result agrees with previous reports of literature [33,38].

On the other hand, molecular adsorption of H_2S on the O-defective $Ce_{0.963}Pr_{0.037}O_{2-x}$(111) surface is an exothermic process. The molecular interaction of H_2S is followed by a dehydrogenation process: $H_2S \rightarrow SH + H$, which occurs over the O1-hole with almost no energy barrier. Furthermore, the electronic structure of the HS-H/$Ce_{0.963}Pr_{0.037}O_{2-x}$(111) system reveals that the H–SH bond was heterolytically broken into H^+ and HS^- species.

4. Conclusions

Our DFT+U calculations reveal a key role of Pr dopant during H_2S interactions on ceria surface. Although, molecular H_2S interactions on the undoped ceria surface are very weak, on the oxygen deficient $Ce_{0.963}Pr_{0.037}O_{2-x}$(111) surface the H_2S molecule easily dehydrogenates into HS^- and H^+ species. The HS^- fragment can bond to either reduced Pr^{3+} or Ce^{3+} cations, while the H^+ fragment bonds to the nearest lattice oxygen anion forming a surface hydroxyl. Our findings indicate that Pr dopant promotes the H_2S dehydrogenation process and, thus, can help to develop new ceria-based supports capable to effectively mitigate sulfur poisoning of the Ni metal active phase.

Acknowledgements

The authors acknowledge the Universidad de Buenos Aires (UBACyT-20020150100095BA) and ANPCyT (FONCYT-PICT-2011-1312) for their financial support.

References

[1] M. Balat. Int. J. Hydrogen Energy 2009, 34, 3589–603.

[2] C.P. Sigar, S.L. Soni, J. Mathur, D. Sharma. Energy Source A 2009, 31,139–48.

[3] E. Kirtay. Energy Conversion and Management 2011, 52, 1778–1789.

[4] L. Sánchez-Silva, D. López-González, A.M. Garcia-Minguillan, J.L. Valverde, Bioresource Technol. 2013, 130, 321–331.

[5] S. Chiu, C. Kao, M. Tsai, S. Ong, C. Chen, C.S. Lin. Bioresour. Technol. 2009, 100, 833 (1–8).

[6] W. Peng, Q. Wu, P. Tu, J. Appl. Phycology 2001,13, 5–12.

[7] L. Rodolfi, G. Zitelli, N. Bassi, G. Padovani, N. Biondi, G. Bonini, M. Tredici. Biotechnol. Bioeng. 2009, 102, 100 (1–12).

[8] P. Schenk, S. Thomas-Hall, E. Stephens, J. Mussgnug, C. Posten, O. Kruse, B. Hankamer. Bio-energy Res. 2008, 1, 20–43.

[9] J. Haase. J. Phys.: Condens. Matter 1997, 9, 3647.

[10] S.L. Lakhapatri, M.A. Abraham. Appl. Catal. A: Gen 2009, 364, 113–121.

[11] J.M. Thomas, W.J. Thomas. *Principles and Practice of Heterogeneous Catalysis*, in: VCH, New York (1997).

[12] Ch. Luo, W. Wang, M. Qiao, K. Fan. J. Molec. Catal. A: Chem 2002,184, 379–.

[13] C.H. Bartholomew, P.K. Agrawal, J.R. Katzer. Adv. Catal. 1982, 31, 135–242.

[14] R.M. Navarro, M.A. Peña, J.L.G. Fierro. Chem. Rev. 2007, 107, 3952–3991.

[15] A. McCoy, M.J. Duran, A-M. Azad, S. Chattopadhyay, M.A. Abraham. Energy & Fuels 2007, 21, 3513–3519.

[16] Z. Chafi, N. Ouafek, E. Boudjennad, N. Keghouche, C. Minot, Sciences & Technologie A 2010, 32, 15–20.

[17] F. Passos, E. de Oliveira, L. Mattos, F. Noronha. Catal. Today 2005, 101, 23–30.

[18] B. Milberg, A. Juan, B. Irigoyen. Appl. Surf. Sci. 2017, 401, 206–217.

[19] L. Eyring, *Handbook on the Physics and Chemistry of Rare Earths*, in: K.A. Gschneider, L. Eyring (Eds.), North-Holland, Amsterdam, 1979.

[20] J.C. Conesa, Surf. Sci. 1995, 339, 337–352.

[21] M. Nolan, S. Grigoleit, D.C. Sayle, S.C. Parker, G.W. Watson, Surf. Sci. 2005, 576, 217–229.

[22] N.V. Skorodumova, M. Baudin, K. Hermansson, Phys. Rev. B 2004, 69, 075401.

[23] G. Kresse, J. Furthmuller, Comput. Mater. Sci. 1996, 6, 15.

[24] G. Kresse, J. Hafner, J. Phys. Rev. B: Cond. Matt. Mat. Phys. 1993, 47, 558.

[25] H. Monkhorst, J. Pack, Phys. Rev. B 1976, 13, 5188–5192.

[26] M. Nolan, S. Grigoleit, D.C. Sayle, S.C. Parker, G.W. Watson, Surf. Sci. 576(2005) 217–229.

[27] H. Li, H. Wang, X. Gong, Y. Guo, Y. Guo, G. Lu, P. Hu, Phys. Rev. B 2009, 79, 193401 (1–4).

[28] C. Castleton, J. Kullgren, K. Hermansson, J. Chem. Phys 2007, 127, 244704 (1–11).

[29] Y. Tang, H. Zhang, L. Cui, C. Ouyang, S. Shi, W. Tang, H. Li, J. Lee, L. Chen, Phys.Rev. B 2010, 82, 125104 (1–9).

[30] R.F.W. Bader. Chem. Rev. 1991, 91 (5), 893–928.

[31] W. Tang, E. Sanville, G. Henkelman. J. Phys. Condens. Matter 2009, 21 (8), 84204.

[32] G. Henkelman, A. Arnaldsson, H. Jónsson, Comput. Mater. Sci. 2006, 36, 354–360.

[33] Hsin-Tsung Chen, YongMan Choi, Meilin Liu, M. C. Lin. J. Phys. Chem. C 2007, 111, 11117–11122.

[34] Y. Tang, H. Zhang, L. Cui, C. Ouyang, S. Shi, W. Tang, H. Li, J. Lee, L. Chen. Phys. Rev. B 82 (2010) 125104 (1–9).

[35] A. Hartridge, M.G. Krishna, A.K. Bhattacharya, Mater. Sci. Eng. B 57 (1999)173–178.

[36] N.V. Skorodumova, S.I. Simak, B.I. Lundqvist, I.A. Abrikosov, B. Johansson. Phys. Rev. Lett. 2002, 89, 166601 (1–4).

[37] Z.-Y. Pu, J.-Q. Lu, M.-F. Luo, Y.-L. Xie, J. Phys. Chem. C 2007, 111, 18695–18702.

[38] A.D. Mayernick, R.Li, K.M. Dooley, M.J. Janik. J. Phys. Chem. C 2011, 115, 24178–24188.